# 2 Light dependence of calcium and membrane potential measured in blowfly photoreceptors in vivo


## *Abstract*

Light adaptation in insect photoreceptors is caused by an increase in the cytosolic $Ca^{2+}$ concentration ($Ca_i$). To better understand this process, we measured $Ca_i$ in vivo as a function of adapting light intensity in the white-eyed blowfly mutant *chalky*. We developed a technique to measure $Ca_i$ under conditions as natural as possible. The calcium indicator dyes Oregon Green 1, 2 or 5N were iontophoretically injected via an intracellular electrode into a photoreceptor cell in the intact eye; the same electrode was also used to measure the membrane potential. The blue-induced green fluorescence of these dyes could be monitored by making use of the optics of the facet lens and the rhabdomere waveguide. The use of the different $Ca^{2+}$-sensitive dyes that possess different affinities for $Ca^{2+}$ allowed the quantitative determination of $Ca_i$ in the steady state. Determining $Ca_i$ as a function of the adapting light intensity shows that $Ca_i$ is regulated in a graded fashion over the whole dynamic range where a photoreceptor cell can respond to light. When a photoreceptor is adapted to bright light, $Ca_i$ reaches stable values higher than 10 $\mu$M. The data are consistent with the hypothesis that the logarithm of the increase in $Ca_i$ is linear with the logarithm of the light intensity. From the estimated values of $Ca_i$ we derive that the $Ca^{2+}$-buffering capacity is limited. The percentage of the $Ca^{2+}$ influx that is buffered gradually decreases with increasing $Ca_i$. At $Ca_i$ levels above 10 $\mu$M, buffering becomes minimal.



The research presented in this Chapter has been published as:
Oberwinkler J, Stavenga DG (1998) J Gen Physiol 112:113-124.

## Introduction

The cytosolic free concentration of $Ca^{2+}$ ions ($Ca_i$) is one of the most important regulation factors in biological cells, influencing a great number of cellular processes. This holds particularly for insect photoreceptor cells, where $Ca_i$ has been shown to play a key role in the regulation of the light-sensitivity (Bader et al., 1976; Autrum, 1979; Muijser, 1979; Tsukahara, 1980; Walz, 1992). More specifically, $Ca_i$ has been implicated in the control of numerous cellular processes in fly photoreceptors, e.g., in the modulation of the light-activated ion-channels (Hardie, 1991a, 1995a, b; Hardie and Minke, 1994b), the activation of the $Na^+/Ca^{2+}$ exchanger (Hardie, 1995a, b), the regulation of many enzymes involved in the transduction cascade (revs: Selinger et al., 1993; Minke and Selinger, 1996; Montell, 1999), the activation of mitochondria (Fein and Tsacopoulos, 1988; Mojet et al., 1991), and the migration of pigment granules in the photoreceptor cells (Kirschfeld and Vogt, 1980; Howard, 1984; Hofstee and Stavenga, 1996).

$Ca_i$ has been reported to rise in insect photoreceptors cells during light stimulation (Howard, 1984; Hardie, 1991a, 1996a; Peretz et al., 1994b; Ranganathan et al., 1994; Walz et al., 1994). In fly photoreceptors, the main part of this increase in $Ca_i$ is caused by the influx of extracellular $Ca^{2+}$ through the light-activated channels (Howard, 1984; Hardie, 1991a, 1996a; Hardie and Minke, 1994b; Peretz et al., 1994b; Ranganathan et al., 1994). Therefore, in an intact eye $Ca_i$ will not only depend on processes inside the photoreceptors themselves, but also on the ionic conditions in the extracellular space. With respect to $Ca^{2+}$, these can vary considerably (Sandler and Kirschfeld, 1988, 1991; Ziegler and Walz, 1989; Rom-Glas et al., 1992; Peretz et al., 1994a).

In the past, $Ca_i$ of insect photoreceptors and its dynamic regulation has been measured either in isolated ommatidia (Peretz et al., 1994b; Ranganathan et al., 1994; Hardie, 1995a, 1996a,b) or in slice preparations of the retina superfused with Ringer solutions (Coles and Orkand, 1985; Hochstrate and Juse, 1991; Walz et al., 1994). Both of these techniques are likely to strongly influence the extracellular ion concentrations and hence to affect $Ca_i$. In an alternative approach, the light dependence of the $Ca^{2+}$ homeostasis in insect photoreceptors has been studied via measurements of the $Ca^{2+}$ concentration in the extracellular space (Sandler and Kirschfeld, 1988, 1991, 1992; Rom-Glas et al., 1992; Peretz et al., 1994a); however, the possibly strong influence of intracellular $Ca^{2+}$ buffering (Hardie, 1996a) and of

$Ca^{2+}$ release from intracellular stores (Walz et al., 1995; Hardie, 1996b; Cook and Minke, 1999) on $Ca_i$ could not be studied in this way.

To better understand the regulation of $Ca_i$ under natural, physiological conditions, we developed a technique to directly measure $Ca_i$ in the intact eye, by using fluorescent $Ca^{2+}$ indicator dyes with varying affinity for $Ca^{2+}$. We thus were able to estimate $Ca_i$ as a function of adapting light intensity. We find that bright illumination of fly photoreceptors causes surprisingly high levels of $Ca_i$, probably even exceeding 10 $\mu$M.

## Materials and Methods

PREPARATION All experiments were performed on female blowflies (*Calliphora vicina*, white-eyed mutant *chalky*) taken from a laboratory culture. The mutant *chalky* was chosen because screening pigments and a functional pupil mechanism are lacking. The animals were immobilized with wax and a small hole was cut in the cornea that was immediately sealed with silicon grease. A silver wire was placed as reference electrode in the same eye. The intactness of the optics of the eye was checked before and after preparation, by inspecting the deep pseudopupil (Franceschini and Kirschfeld, 1971). The animal was placed in a holder that allowed adjustment of its orientation. The holder with the animal was then positioned on the micromanipulator-controlled stage of a Leitz Orthoplan epi-fluorescence microscope.

ELECTROPHYSIOLOGY Conventional electronic equipment was used to measure the intracellular membrane potential and to pass current through the electrode (Axoclamp 2A, Axon Instr.; operated in bridge mode). The electrodes were pulled on a P-87 (Brown and Flaming, Sutter Instr.) from borosilicate glass (1.5 mm outer diameter, 0.86 mm inner diameter, Clark Instr.), and their tip was filled with a solution containing 5 mM of calcium indicator dye (Oregon Green 1, 2 or 5N, Molecular Probes, in the following abbreviated as OG1, OG2 and OG5N, respectively) in 0.1 M KCl. The shank was then backfilled with 0.1 M KCl solution. The electrodes had a resistance of 150-250 M$\Omega$ in the tissue. The procedure of electrical recording was as follows. First, the tip of the electrode was adjusted at the optical axis of the objective, at a level 150 $\mu$m below the focal plane. The stage of the microscope with the fly in the holder was then moved under the objective, so that the electrode penetrated the eye through the hole at a level 150 $\mu$m below the corneal surface and the fly was advanced so far that a penetrated cell was approximately co-axial with the objective.

DYE FILLING After impalement, the cell was dye-filled by applying pulses of $-1.2$ to $-2.2$ nA at 0.5 Hz (50% duty cycle). The process of filling lasted at most 5 min, but was usually complete after 1-2 min. Sometimes no current was necessary, because cells filled simply by diffusion of the dye from the tip of the electrode. The filling of a cell was immediately apparent from the distinct fluorescence emerging from one of the facet lenses. As outlined in the Results, excessive concentrations of the dye induced alterations of the electrical response of the photoreceptor cells. Therefore, as a precaution, the process of dye filling was checked in regular intervals by visually judging the intensity of the fluorescence and filling was stopped when the intensity of the fluorescence reached values sufficient from optical recordings. Recordings of cells that were subsequently found to display alterations in their peak-plateau transitions (indicative of excessive additional $Ca^{2+}$ buffering) were rejected (see Results).

OPTICAL SETUP Two light sources, a 75 W xenon lamp and a 100 W halogen lamp, delivered the test and adapting light beam, respectively. Shutters (Uniblitz, Vincent Associates; rise time $< 3$ ms) and grey filters controlled the light flux in both light paths independently. A 50% mirror combined the beams, which then passed the microscope's fluorescence cube (Leitz DM 510, i.e. blue excitation causing green emission). A 10x objective (NA 0.25, Spindler and Hoyer) projected the blue illumination onto the fly eye. The green emission was measured by a photomultiplier (R928, Hamamatsu). A small diaphragm (diameter 0.2 mm) in the image plane was adjusted so that only the fluorescence emerging from the brightly shining facet lens was selected. The background due to a distinct autofluorescence of the cornea thus was minimized.

DATA ACQUISITION The signals from the electrode amplifier and the photomultiplier were filtered at 2 kHz (Krohn-Hite, model 3343) and sampled at 5 kHz per channel by a CED 1401 interface (Cambridge Electronic Design). Further processing of the data was performed off-line.

PHOTOGRAPHY After filling a cell with OG1 the fly was placed in a fluorescence microscope (Nikon Diaphot) equipped with a Nikon F-601M camera containing a black and white film (Ilford SFX; 200 ASA pushed to 800 ASA). The blue (477 nm) induced green ($>$510 nm) fluorescence was photographed with a dry objective (4x, NA 0.1, Spindler and Hoyer; Figure 2.1) as well

as a water immersion objective (SW25, NA 0.6, Leitz; Figure 2.1c and d). In Figure 2.1a, a halogen light source delivered additional side illumination for recognition of the eye and facet pattern. To identify the stained cell, the eye was first illuminated during 5 s with 380 nm light for creating the highly fluorescent visual pigment state M′ (Stavenga et al., 1984). Then the green (546 nm) induced red emisssion (>580 nm) was photographed (water immersion SW25; Figure 2.1d).

QUANTITATIVE DATA ANALYSIS To estimate $Ca_i$ quantitatively as a function of the adapting light, we first adapted the photoreceptor cells for 5 s to a given light intensity, and then probed the fluorescence with a bright test flash. The fluorescence signal at the beginning of the test flash thus represents the $Ca_i$ signal due to the adapting light. At the end of the test flash the signal is dominated by the $Ca^{2+}$ influx caused by the much brighter test flash. Because we used non ratiometric $Ca^{2+}$ indicators it was necessary to ensure that changes in dye concentration (caused by bleaching or by active transport out of the cell) did not corrupt the measurements. When using the high affinity dyes OG1 or OG2, we therefore took the difference in the fluorescence signal between the beginning and the end of the fluorescence trace for the quantitative analysis. Any change in the magnitude of the fluorescence signal at the end of the test flash, i.e. when the dye is saturated, indicated that the concentration of the dye changed. For the data from OG5N, this procedure was not possible, because due to the low affinity of OG5N for $Ca^{2+}$ the signal does not saturate. We therefore took the difference between the initial fluorescence of the photoreceptor cell adapted to different light intensities and the initial fluorescence signal of the dark adapted photoreceptor cell. This method requires regular checks for changes in the magnitude of the fluorescence signal from the dark adapted photoreceptor. Because the magnitude of the fluorescence signal of our single wavelength dyes depends on the concentration of the dye, we normalized the data in order to be able to compare data from different cells. The quantitative values from a single cell describing the influence of the adapting light were normalized between the value of the lowest adaptation intensity and the value of the highest adaptation intensity, and subsequently plotted as a function of the light intensity. To estimate the dependence of $Ca_i$ on the light intensity, we calculated the expected fluorescence signal as a function of the light intensity with the function $F(Ca_i) = {Ca_i}^h / ({Ca_i}^h + {K_d}^h)$. Since our in vivo method does not allow a direct calibration of the indicators, we used the $K_d$ values published by

Haugland (1996): OG1: $K_d = 0.16$ $\mu$M; OG2: $K_d = 0.58$ $\mu$M; OG5N: $K_d = 20$ $\mu$M. Hill-coefficients were taken equal to 1, except for OG5N, for which repeatedly Hill-coefficients lower than one have been reported (e.g. Ukhanov et al., 1995); we used a value of 0.7, derived from fitting the data published for Calcium Green 5N (Haugland, 1996). Using this function, we calculated the expected fluorescence as a function of the light intensity, for functions of $Ca_i$ depending on the light intensity. The resulting functions of fluorescence depending on the light intensity were normalized (again between the value for the lowest light intensity and the value for the highest light intensity, i.e. between $\log I = -3$ and $\log I = 2$), to allow comparison with the measured data.

## Results

### A new method to measure cytosolic $Ca^{2+}$ dynamics in photoreceptors of insect compound eyes in vivo

The preferred method for recording the membrane potential of individual insect photoreceptors in intact animals is to insert an electrode through a small hole in the cornea and to subsequently impale a photoreceptor cell. Here we demonstrate that this technique can also be used to inject calcium indicator dyes into a penetrated cell. Figure 2.1a shows an eye of a blowfly where one cell was dye-filled, photographed through a dry objective. One facet lens clearly shines up. Neutralizing the cornea by using a water immersion objective (Kirschfeld and Franceschini, 1969) allows examination of the subcellular distribution of the dye, because it is then possible to focus onto the tips of the rhabdomeres and the cell bodies; Figure 2.1b depicts this optical situation diagramatically (for a detailed account of the anatomy of the fly retina see Hardie, 1985). Figure 2.1c shows the blue-induced green fluorescence of the stained cell. Both the soma and rhabdomere of one of the photoreceptor cells fluoresce, indicating that the dye is distributed throughout that photoreceptor cell and that part of the excited fluorescence is efficiently guided by the rhabdomere. To visualize the localization of the stained cell within the ommatidial lattice of the fly's eye, we exploited the bright red fluorescence of the M′ state of the visual pigments (Stavenga et al., 1984, see Materials and Methods) when illuminated with green light. The green-induced red fluorescence (Figure 2.1d) of the same part of the retina as in Figure 2.1c shows the rhabdomere of the stained cell (arrow), an R5 cell, and the regular pattern of fluorescing rhabdomeres; of course, the green-induced red fluorescence of the dye is much weaker than the blue-induced green fluorescence.

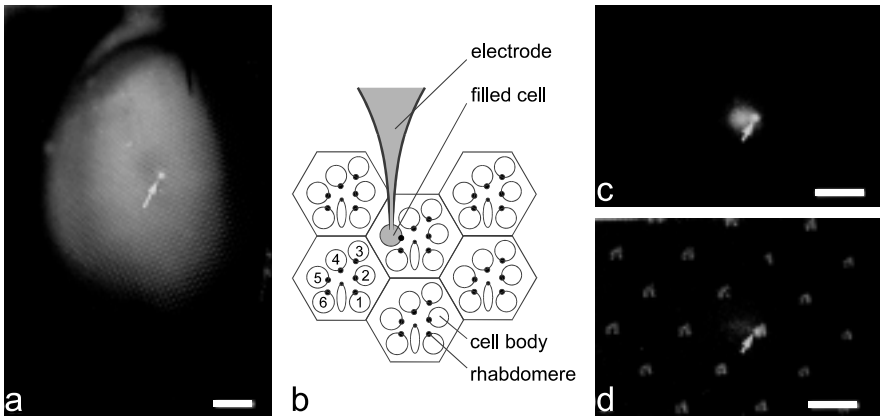


FIGURE 2.1: Photographs of a dye injected photoreceptor cell. a) Left eye of a white-eyed mutant blowfly *Calliphora vicina* photographed with a dry objective. The facet lens overlying the dye-injected cell clearly shines up (scale bar 0.2 mm). b) Diagram of the photoreceptor organization and the recording situation after optically neutralizing the cornea with a water immersion objective (Kirschfeld and Franceschini, 1969). c) Blue-induced green fluorescence photographed through a water-immersion objective, showing that the rhabdomere and the cell body of the stained cell fluoresce. d) Green-induced red fluorescence of the same eye region showing the characteristic pattern of the rhabdomeres; one rhabdomere -belonging to the stained cell- is brighter than the others (arrow), allowing to identify the stained cell as an R5 photoreceptor (scale bar in c) and d) 20 $\mu$m).

Under the physiological optical conditions used in the experiments, light emitted from the rhabdomere leaves the eye within an angle of 1-2° (van Hateren, 1984), while the fluorescence coming from the cell body is expected to irradiate from the cornea within an angle of $\sim$11° (assuming a diameter of the cell of $\sim$10 $\mu$m and a focal distance of 50 $\mu$m of the facet lens). Because the objective aperture is $\sim$14°, the photomultiplier samples a mixture of light emitted by the rhabdomere and the cell body; however, the ratio of the amount of light sampled from the two cellular compartments depends on the precise alignment of the investigated cell's visual axis with the microscope objective. This inevitably varied from one recording to another.

From such a dye-filled cell, we recorded simultaneously the light-induced changes of the membrane potential and the accompanying fluorescence, using the low affinity dye OG5N (Figure 2.2). As in all experiments presented here, the cell was dark adapted for 1 min before and between the recordings. Illumination causes, after a delay of a few ms, a rapid depolarization

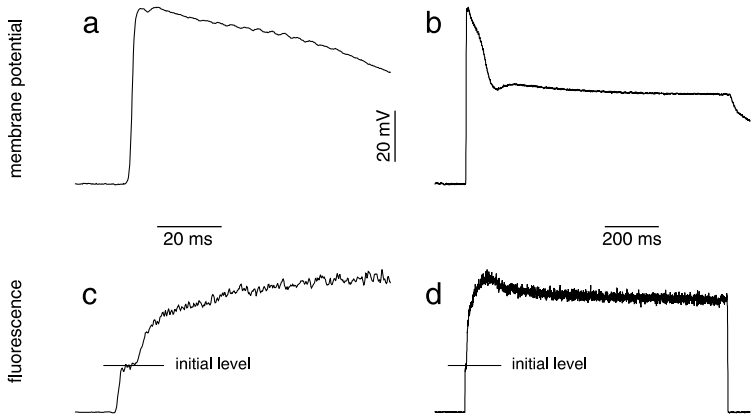


FIGURE 2.2: Simultaneous recording of membrane potential (a, b) and $Ca^{2+}$ induced fluorescence (c, d) from a dark adapted photoreceptor illuminated with saturating light. The same data are shown with high (a, c) and with low temporal resolution (b, d). The cell was injected with the low affinity dye OG5N. The fluorescence signal increases very fast after opening the shutter and peaks after ~100 ms before levelling off towards a plateau. The depolarization of the membrane, however, displays still faster kinetics. All traces are averages of 9 recordings.

of the cell membrane, reaching a peak after ~10 ms (Figure 2.2a); subsequently, the receptor potential levels off to a plateau value (Figure 2.2b). The blue-induced green fluorescence appears to follow a similar, although somewhat slower time course. First, during the opening of the shutter the fluorescence signal rises to an initial plateau (initial level, Figure 2.2c, d). This is the sum of tissue autofluorescence and fluorescence of the dye due to resting $Ca_i$. Then, after a short delay (~3 ms), the emission very rapidly increases, indicating an abrupt rise in $Ca_i$ (Figure 2.2c). The peak occurs after ~100 ms, and the subsequent decrease to a plateau of the fluorescence distinctly lags that of the receptor potential (Figure 2.2d).

### *The effect of the $Ca^{2+}$ indicator dyes on the membrane potential*

All $Ca^{2+}$ indicator dyes are also $Ca^{2+}$ buffers. Increasing the intracelluar $Ca^{2+}$ buffering capacity by introducing the dyes can considerably alter the dynamics and the regulation of $Ca_i$ (e.g. Neher, 1995). Because fly photoreceptors are thought to react sensitively to changes in the $Ca^{2+}$ homeostasis (Muijser, 1979; Hardie, 1995b) we checked for changes in the waveform of

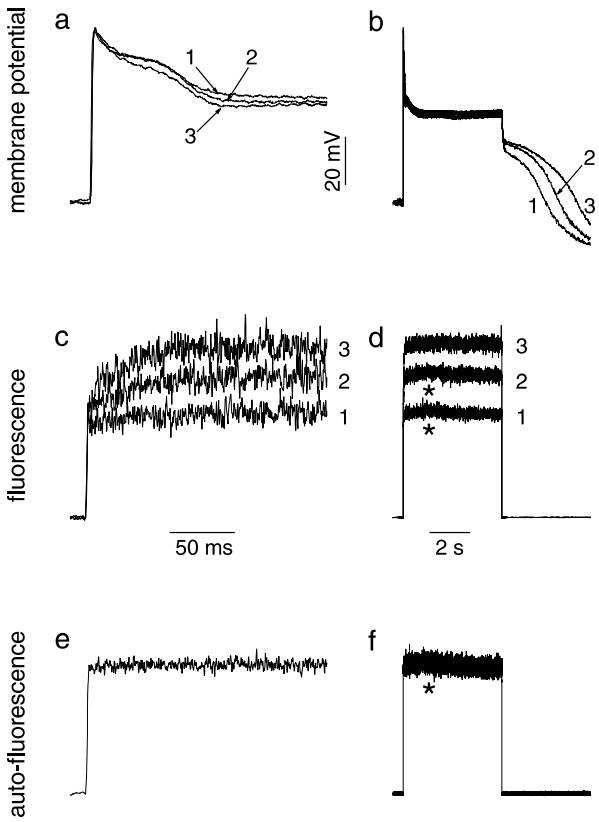


FIGURE 2.3: The effects of dye filling on the membrane potential. The photoreceptor cell was impaled with an electrode containing OG2 and then filled without applying current. Traces 1, 2 and 3 were measured 1 min, 4 min and 6 min after impalement, respectively, by a 1 s stimulus of saturating intensity. While the fluorescence signal (c, d) increases with time of impalement, indicative for an on-going dye-loading, the membrane potential response (a, b) of the cell during the light stimulus is hardly changed. Only after turning the stimulus off, a distinct prolongation of the depolarizing afterpotential can be seen, due to an increase in the concentration of the dye (b). The fluorescence traces in d) are smoothed by adjacent averaging with a window size of 20 sample points (equivalent to 4 ms) and therefore the rising phase that is visible in c) is not discernible in d). The traces in e) and f) were obtained from a different preparation in which no cell had been dye-filled; these traces are averages of 5 recordings. They show that the tissue autofluorescence is essentially constant, except for a small, transient increase in fluorescence signal ($\star$) that can be attributed to a light induced change in redox state of mitochondrial flavoproteins (Stavenga and Tinbergen, 1983).

the membrane potential due to loading with the dyes. The cell of Figure 2.3 spontaneously filled with OG2, i.e. without the need to apply current. The first measurement was taken at ∼1 min after impalement of the cell, the following after 4 and 6 min, respectively. The fluorescence signal (Figure 2.3c, d) increased with time, indicating that the cell progressively took up more of the dye. Following light-off, the time course of the afterdepolarization became prolonged. The afterdepolarization is -at least partially- caused by the $Na^+/Ca^{2+}$ exchanger (Hochstrate, 1991), which in *Calliphora* photoreceptor cells can generate currents stronger than 1 nA (Gerster, 1997). Therefore, the prolongation of the afterpotential indicates that the $Na^+/Ca^{2+}$ exchanger extrudes more $Ca^{2+}$ when the dye concentration increases. This is in line with an increased buffering of $Ca^{2+}$ ions by the dye, which leads to an increase in the total concentration of $Ca^{2+}$ at comparable concentrations of free $Ca^{2+}$. We consistently found that the dyes prolonged the duration of the afterdepolarization, even at concentrations that were difficult to detect photometrically. However, the waveform of the receptor potential during light-on remained virtually unchanged (Figure 2.3a, b), suggesting that the rising dye concentration did not appreciably affect the phototransduction process.

Generally, the effect of the dye on the membrane potential during the light stimulus was inconspicuous, but peak values sometimes increased by a few mV after filling the cell; in some cases the peak to plateau transition of the membrane potential at the onset of light stimulation was accelerated after dye filling. When cells were filled too much, the typical reduction of the peak-plateau transition, caused by a substantial increase in $Ca^{2+}$ buffering (Bader et al., 1976; Muijser, 1979; Tsukahara, 1980; Walz et al., 1994) could be observed; these cells then were rejected.

In addition to the fluorescence from the dyes, we measured the tissue autofluorescence from an eye of which no cell was injected with a $Ca^{2+}$ indicator. This tissue autofluorescence remained essentially constant upon illumination (Figure 2.3e, f). Nevertheless, occasionally a very slight, transient increase in autofluorescence could be noticed in this background ($\star$ in Figure 2.3f), probably due to the light-induced, transient redox changes of the flavoproteins in the photoreceptor mitochondria (Stavenga and Tinbergen, 1983; Mojet et al., 1991). Sometimes, such a small increase in fluorescence also was observed when measuring from a cell filled with the high affinity dyes, i.e. in Figure 2.3d ($\star$); this small increase might also be attributable to the observed increase of the autofluorescence, that is, to transient changes in the redox state of the flavoproteins. In the processed experiments, this variation

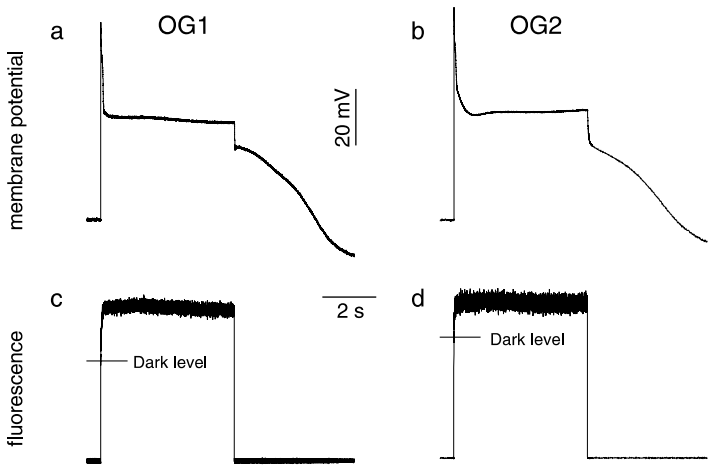


FIGURE 2.4: Membrane potential (a, b) and fluorescence (c, d) signal from two cells injected with the high affinity dyes OG1 (a, c) and OG2 (b, d), respectively. The dark adapted cells were illuminated for 5 s with light of saturating intensity. The fluorescence signal increases monotonically upon stimulation and does not display the peak that can be seen when using the low affinity dye OG5N (Figure 2.2). This indicates that the high affinity dyes OG1 and OG2 are saturated by the levels of $Ca_i$ reached under bright illumination. This implies that in these conditions $Ca_i$ exceeds 10 $\mu$M, the concentration where OG2 saturates (Haugland, 1996). Traces in a) and c) are averages of 5 recordings, traces in b) and d) are averages of 7 recordings.

in the background signal was fully negligible compared to the light-induced changes in dye fluorescence.

### *Bright light causes $Ca_i$ to increase into the high micromolar range*

Fluorescence measurements of cells injected with the low affinity dye OG5N ($K_d = 20$ $\mu$M; Haugland, 1996) yielded somewhat variable results. The time to peak ranged from 100 ms to almost 1 s; the time required for reaching a stable plateau takes 2-4 s. This variability might be the result of slight differences in the alignment of the investigated cells. Because the $Ca^{2+}$ influx occurs in the rhabdomeres, and the $Ca^{2+}$ ions diffuse from the rhabdomere into the cell body rather slowly (Ranganathan et al., 1994), a variation in the ratio of light sampled from the rhabdomere and from the cell body could cause a variation in the observed time course of the fluorescence signal.

No peak in the fluorescence signal was observed when high affinity dyes (OG1 or OG2; $K_d$ = 0.16 $\mu$M and 0.58 $\mu$M, respectively; Haugland, 1996) were used (Figure 2.4a, b). The fluorescence signal then increased monotonically towards a stable plateau that was reached after 100-400 ms. These findings are fully consistent with the difference in affinity for $Ca^{2+}$ of the dyes used, suggesting that $Ca_i$ attains values where the high affinity dyes OG1 and OG2 are saturated. Because OG2 saturates at $Ca_i \approx 10$ $\mu$M (Haugland, 1996), $Ca_i$ exceeds this range during the peak observed with the low affinity dye OG5N.

### *Steady state $Ca_i$ after adaptation to different light intensities*

To measure the dye fluorescence with an acceptable signal to noise ratio, it is necessary to use very high light intensities. To assess $Ca_i$ at moderate and intermediate intensities, we employed a double pulse paradigm, where an adapting light stimulus was followed by a bright test flash. We adapted the photoreceptors for 5 s at a given intensity, and then probed the fluorescence with a short (0.2-0.5 s) test flash. An adaptation time of 5 s was considered sufficient, because both the stability of the membrane potential and the fluorescence measurements indicated that after 5 s $Ca_i$ reached a stable plateau value and that diffusion of the $Ca^{2+}$ ions had reached an equilibrium. We assume, therefore, that the subcellular distribution of $Ca_i$ in the cytosol is fairly homogeneous after 5 s.

Figure 2.5 shows an example of such an experiment. The high affinity dye OG1 was used. The fluorescence signal at the beginning of the bright test flash increases with increasing adapting light intensity in the low intensity range, but it saturates at high intensities. Again, we confirmed that this is caused by saturation of the dye by using the low affinity dye OG5N. This dye reports an increase in $Ca_i$, even up to the highest intensities used (see below).

We repeated the experiment of Figure 2.5 with all three dyes (OG1, OG2, OG5N) in nine cells (three for each dye) from six animals. Figure 2.6 summarizes the experiments. In order to correct for the different absolute sensitivities of the different cells, the $V/\log I$ curve of the peak receptor potential of each cell was fitted separately to a logistic function: $V = V_{\max} I^n/(I^n+1)$ (Laughlin, 1981). The light intensity $I$ is taken here relative to the light intensity that causes a half maximal peak depolarization; this intensity was assigned the value $\log I = 0$. Furthermore, the potential values were normalized to the maximal peak depolarization ($V_{\max}$). Figure 2.6a presents the

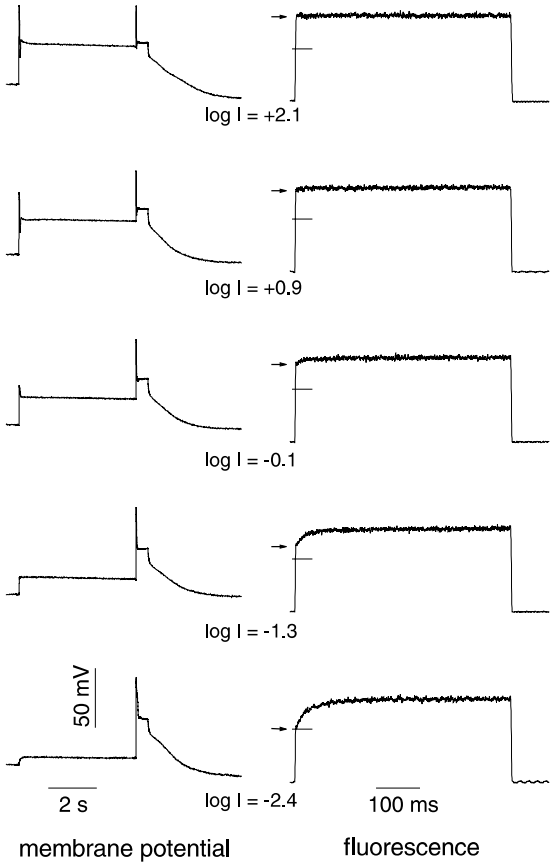


FIGURE 2.5: Example of the double pulse experiments used to determine $Ca_i$ as a function of light intensity. Membrane potential traces are given in the left hand column. The dye-injected (OG1) and dark-adapted cell was stimulated with an adapting light (5 s), the intensity of which is indicated for each experiment. Intensities are expressed relative to the light intensity that caused a half maximal peak depolarization; this intensity was assigned the value $\log I = 0$. After adapting for 5 s, the level of $Ca_i$ was probed with a bright test flash (500 ms). The fluorescence signal measured during this test flash is shown in the right hand column on an expanded time scale. The horizontal line at the beginning of the fluorescence traces indicates the initial fluorescence value when no adapting light was given. With increasing adapting intensity, the initial value of the fluorescence (indicated by arrows) increases. At the highest adapting intensities used, no increase in fluorescence can be observed during the test flash due to saturation of the high affinity dye OG1. All traces shown are averages of 5 recordings.

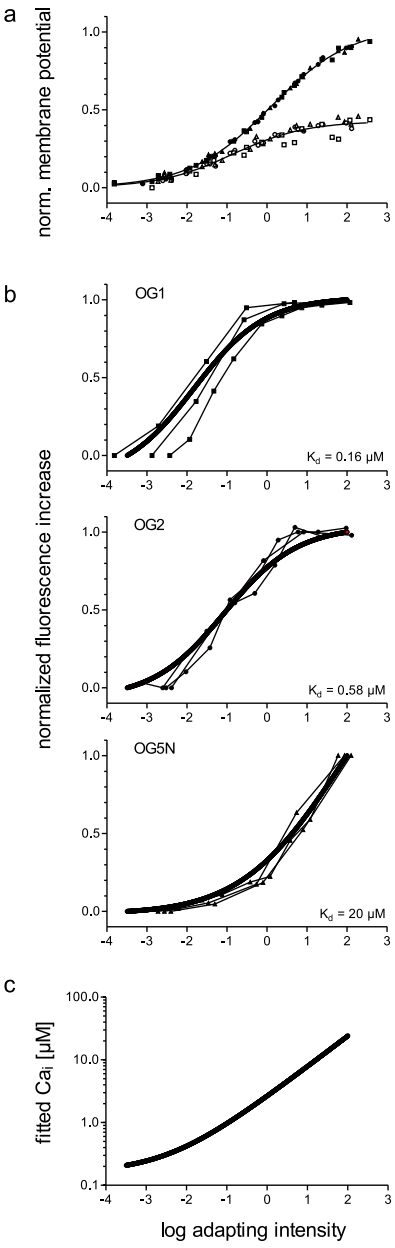


FIGURE 2.6: Summary of the double pulse experiments. a) Normalized depolarization of the peak (filled symbols) and plateau (open symbols) of the membrane potential are given as a function of adapting light intensity. The smooth curves are obtained by fitting the logistic function $V = V_{\max} I^n/(I^n+1)$ to the experimental data (exponent $n = 0.45$ for peak values and 0.47 for plateau values; the normalized $V_{\max}$ for plateau values was fitted to be 0.43). The light intensity $I$ is taken relative to the light intensity that causes a half maximal peak depolarization; this intensity was assigned the value $\log I = 0$. b) Normalized fluorescence increase caused by the adapting light for the three dyes used (symbols connected by thin lines); data from three different cells are shown for each dye. Normalization procedures for all panels are explained in Materials and Methods. The membrane potential and fluorescence data obtained with a specific dye are indicated with the same symbol. The fluorescence increase reported by OG1 and OG2 rises with increasing adapting light intensity and saturates at bright light. The signal that was obtained with OG5N continues to increase up to the highest intensities. This shows that $Ca_i$ is regulated in a graded fashion over the whole intensity range and that $Ca_i$ levels exceed 10 $\mu$M at high light intensities. The bold lines are fits to the experimental data obtained by calculating the fluorescence ($F$) as a function of $Ca_i$ according to $F(Ca_i) = {Ca_i}^h / \left({Ca_i}^h + {K_d}^h\right)$ and normalizing, as detailed in the Materials and Methods section. $Ca_i$ was assumed to increase with a simple power function of adaptation light intensity yielding the curve shown in c) (see Results).

resulting peak and plateau values as a function of relative light intensity. The $V_{\max}$ values ranged for the peak from 60 to 82 mV (average 72 $\pm$ 6 mV SD) and for the plateau from 19 to 40 mV (average 30 $\pm$ 6 mV SD); the exponent $n$ for the peak values ranged from 0.40 to 0.47 (average 0.44 $\pm$ 0.02 SD) and for the plateau values from 0.42 to 0.58 (average 0.50 $\pm$ 0.05 SD). The $V/\log I$ curves appeared to be homogeneous and are fully consistent with similar measurements reported in the literature (Laughlin and Hardie, 1978; Matić and Laughlin, 1981; Sandler and Kirschfeld, 1988; Roebroek and Stavenga, 1990); this suggests again that the dyes did not seriously affect the membrane potential. The fluorescence signals measured during the test flashes were evaluated quantitatively as described in Materials and Methods. Figure 2.6b shows the resulting dependency of the fluorescence signal on the adapting light intensity for the three different dyes.

Obviously, the results for the high affinity dyes OG1 and OG2 are quite different from those for OG5N (Figure 2.6b). While the signals obtained with OG1 or OG2 both show saturation, the signal obtained with OG5N increases with light intensity even up to the highest intensities used. In addition, while the signals of OG1 and OG2 already show a pronounced increase at the lowest intensities, with OG5N this occurs only at $\log I \geq 0$. The differences between OG1 and OG2 are rather inconspicuous. Mainly, OG1 seems to become activated in average at intensities half a log-unit lower than OG2, as can be seen from the leftward shift in the activation curves of OG1 with respect to the curve of OG2. Taken together, the important findings of these experiments are (1), that $Ca_i$ is regulated over the whole intensity range where the photoreceptor can respond to light, and (2), that OG1 and OG2 are saturated at intensities about one log-unit above the intensity for half-maximal activation of the peak membrane potential. This demonstrates that at bright adaptation intensities, the plateau values of $Ca_i$ exceed 10 $\mu$M, the saturation value of OG2 (Haugland, 1996).

The slope of the fluorescence vs $\log I$ plots is almost linear in the low intensity region for OG1, in the region between $\log I = -2$ to $\log I = 0.5$ for OG2 and in the high intensity region for OG5N. This seems to imply that log $Ca_i$ rises linearly with $\log I$. To get a more quantitative picture of the changes of $Ca_i$ caused by light adaptation, we have therefore tried to describe the dependency of $Ca_i$ on the light intensity with a simple power function: $Ca_i(I) = Ca_{i,da} + aI^b$; $Ca_{i,da}$ denotes here $Ca_i$ in the dark-adapted state, assumed to be 0.16 $\mu$M, the value found for *Drosophila* (Hardie, 1996a). The experimental data were then fitted by taking $a = 2.5$ $\mu$M and $b = 0.5$, resulting in the curve shown in Figure 2.6c; the bold lines in Figure 2.6b represent

the simulated fluorescence values, calculated as described in the Materials and Methods section. The similarity between measured and simulated data suggests that the function chosen for describing $Ca_i$ is appropriate. As shown in Figure 2.6c, at $\log I = 2$, $Ca_i$ equals 25 $\mu$M. We are well aware that the accuracy of this approach is limited. With slight variations of the parameters a and b, reasonable good fits can still be obtained, whilst yielding considerably different values for $Ca_i$, especially for high light intensities. It was no longer possible to obtain a good fit between the simulated fluorescence functions and our data, when the parameter $a$ was chosen smaller than 2 or the parameter $b$ smaller than 0.5. Yet even with this combination of parameters, $Ca_i$ at $\log I = 2$ is still estimated reach 20 mM. Therefore, the values of Figure 2.6c can be considered to be a conservative estimate. The value for $Ca_{i,da}$, the dark adapted $Ca_i$, influences the simulated fluorescence curves neglibly, and it was thus not possible to estimate it with our data. We therefore used 0.16 $\mu$M, the value measured in *Drosophila* (Hardie, 1996a) throughout the simulations.

## Discussion

### Measuring calcium in insect photoreceptors

We demonstrate in this Chapter that it is possible to measure the light-induced changes of $Ca_i$ in photoreceptor cells in the intact eye of flies by using fluorescent $Ca^{2+}$ indicators. The fluorescence signal can be measured simultaneously with the light-induced receptor potential. Dye filling causes alterations of the membrane potential (Figure 2.3a, b) that appear to be consistent and at least qualitatively explainable with the buffer action of the dyes. An increase in buffer capacity leads to an increased amount of $Ca^{2+}$ ions to enter the cell before a given concentration is reached. This in turn causes the $Na^+/Ca^{2+}$ exchanger to be activated for a longer period to extrude the extra load of $Ca^{2+}$; the afterdepolarization is therefore prolonged.

Increasing the intracellular buffer capacity by introducing $Ca^{2+}$ buffers normally induces pronounced changes in the light response. The peak to plateau transition is diminished and the response kinetics are slowed down (Bader et al., 1976; Muijser, 1979; Tsukahara, 1980; Walz et al., 1994; Hardie, 1995b). We also observed these effects at high dye loads. However, usually this could be avoided and we carefully checked for these alterations of the waveform. Since the membrane potential is a sensitive measure of photoreceptor function, we conclude that our manipulations have not, or at most weakly, influenced the $Ca^{2+}$ homeostasis during the light response.

### *Changes in $Ca_i$ induced by light stimulation*

Bright light stimulation of insect photoreceptors in isolated ommatidia (Peretz et al., 1994b; Ranganathan et al., 1994; Hardie, 1996a) or perfused eye slices (Walz et al., 1994) rapidly increases $Ca_i$ to high concentrations. In *Drosophila* (Hardie, 1996a) and the drone (Walz et al., 1994), the increase in $Ca_i$ is fast and consistently saturates high affinity dyes after ∼200 ms. Using Mag-Indo-1, Hardie (1996a) estimated that $Ca_i$ reaches values up to 50 $\mu$M in isolated *Drosophila* photoreceptor cells. Here we show that $Ca_i$ reaches similar values in photoreceptor cells of *Calliphora* in vivo (Figures 2.2, 2.4). The saturation of OG2 upon bright illumination indicates that in *Calliphora* $Ca_i$ reaches values exceeding 10 $\mu$M.

The adaptation experiments (Figures 2.5, 2.6) allow to estimate how $Ca_i$ depends on the light intensity (Figure 2.6c). Quantitative measurements of $Ca_i$ with fluorescent indicators are often complicated by the fact that the indicators have different properties in the cytoplasm of cells than in solutions. However, since the $K_d$-values of the indicators only have been reported to increase when the indicator is brought into the cytosol (e.g. Hardie, 1996a), it is unlikely that we overestimated $Ca_i$. We conclude that $Ca_i$ reaches values at least up to 20 $\mu$M when illuminated with the brightest intensity used in this study. Surprisingly, these high values are not only reached during short and local $Ca^{2+}$ peaks, but are maintained after several seconds of light adaptation, implying that these high concentrations are sustained during prolonged periods. The fluorescence signal at high light intensities reaches a stable level after at most 2-4 s (Figures 2.4-2.6), showing that the distribution of $Ca^{2+}$ ions then is in a steady state. In *Limulus*, only the R-lobe shows a dramatic increase in $Ca_i$; this increase is spread over a distance of at least 20 $\mu$m (Ukhanov and Payne, 1995). Therefore it seems likely that high values of $Ca_i$ are also reached in the cell bodies of *Calliphora* photoreceptor cells that have a diameter of ∼10 $\mu$m.

### *Buffering of the $Ca^{2+}$ influx*

The finding that $Ca_i$ reaches very high values is supported by measurements of changes of the extracellular calcium concentration with $Ca^{2+}$-selective electrodes (Sandler and Kirschfeld, 1988). In the drone, the glia cells do not take up $Ca^{2+}$ (Coles and Orkand, 1985) and volume changes in the retina are small (Orkand et al., 1984; Ziegler and Walz, 1989). Assuming that this is also the case in the blowfly, and that there is no substantial $Ca^{2+}$ release from internal stores (Ranganathan et al., 1994; Hardie, 1996a; Cook and Minke,

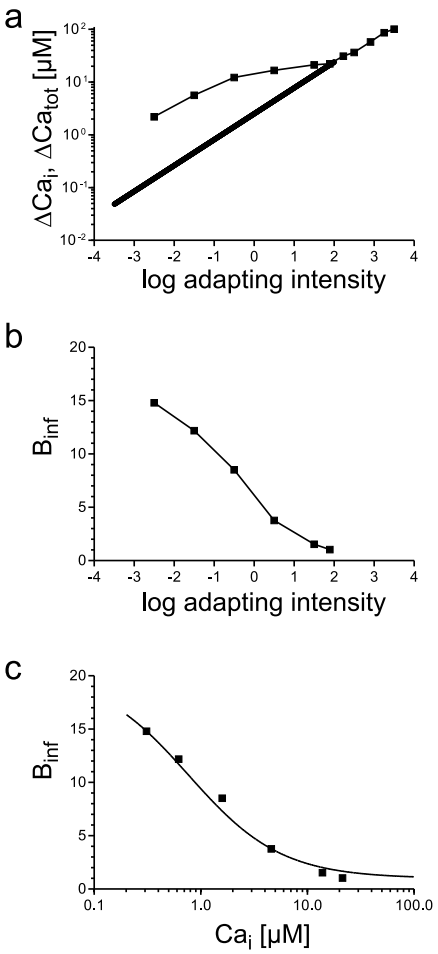


FIGURE 2.7: a) Comparison of changes in $Ca_i$ ($\Delta Ca_i = Ca_i - Ca_{i,da} = aI^b$, continuous bold line, taken from Figure 2.6c) and changes in the total $Ca^{2+}$ concentration ($\Delta Ca_{tot}$, ■) measured by Sandler and Kirschfeld (1988, their Figure 1c). The $\Delta Ca_{tot}$ values were derived using the formula $\Delta Ca_{tot} = \Delta Ca_o/R$. The ratio $R$ between the volume of the photoreceptors and the extracellular space was assumed to be 6.3 (Sandler and Kirschfeld, 1991), and the change in extracellular $Ca^{2+}$ concentration ($\Delta Ca_o$) was calculated assuming that in the dark adapted state the extracellular $Ca^{2+}$ concentration amounts to 1.4 mM (Sandler and Kirschfeld, 1991). At $\log I = 2$ the two curves approximate each other. At lower intensities, however, $\Delta Ca_{tot}$ values are larger than the values obtained with the dyes. This indicates that the influx of $Ca^{2+}$ is buffered. b) Buffering coefficient of the $Ca^{2+}$ influx ($B_{inf} = \Delta Ca_{tot}/\Delta Ca_i$) shown as a function of adapting light intensity. c) Same data plotted as a function of $Ca_i$. The continuous line was obtained by fitting a simple buffer model (see Discussion). The buffering of the $Ca^{2+}$ influx reduces with increasing $Ca_i$, and at $Ca_i$ levels above 10 $\mu$M buffering becomes minimal.

1999) we can calculate from the decrease in extracellular calcium measured by Sandler and Kirschfeld (1988, their Figure 2.1c) the amount of $Ca^{2+}$ entering the photoreceptors ($\Delta Ca_{tot}$; symbols in Figure 2.7a) and compare the resulting values with our estimates of the increase in $Ca_i$ ($\Delta Ca_i$; bold line in Figure 2.7a). The calculated values appear to be in good agreement with the values of the light induced $Ca_i$ increase at $\log I \geq 2$. Both curves have a similar slope at these high intensities.

However, at light intensities below $\log I = 2$, $\Delta Ca_{tot} > \Delta Ca_i$, or, the amount of $Ca^{2+}$ entering the photoreceptor cells from the extracellular space is larger than the increase of $Ca_i$ (Figure 2.7a). This difference can be explained by assuming that the $Ca^{2+}$ influx is buffered, e.g. by uptake in organelles or binding to proteins. The buffering coefficient $B_{inf} = \Delta Ca_{tot}/\Delta Ca_i$ is presented in Figure 2.7b as a function of light intensity, and in Figure 2.7c as a function of $Ca_i$. Clearly, the buffering capacity is limited, and at $Ca_i \geq 10$ $\mu$M (corresponding to $\log I = 1.5$) buffering becomes minor. The values of 10-20 obtained for the buffering coefficient at $Ca_i \leq 1$ $\mu$M are more than an order of magnitude lower than the estimates for photoreceptors of *Drosophila* (Hardie, 1996a) or *Limulus* (O'Day and Gray-Keller, 1989). We note that the obtained buffering values are subject to a number of uncertainties. Firstly, mismatching the stimulation intensities of Sandler and Kirschfeld's (1988) measurements with respect to our experiments might have affected the estimation of the values for $B_{inf}$. In addition, our calculations assume that there is no extracellular $Ca^{2+}$ buffering; the buffering coefficients for the $Ca^{2+}$ influx would be underestimated by the factor of extracellular $Ca^{2+}$ buffering, if this assumption does not hold. Also, if the assumptions of a constant extracellular volume and the non-involvement of the glial cells in the $Ca^{2+}$ homeostasis do not hold, this will obviously modify the quantitative values of $B_{inf}$. However, if $Ca^{2+}$ buffering is assumed to be constant at a high buffering coefficient $B_{inf}$ throughout the light intensity range studied, there would not be enough extracellular $Ca^{2+}$ to sustain a $Ca^{2+}$ influx that causes $Ca_i$ to rise to 20 $\mu$M. We calculate a maximal value for $B_{inf}$ of 11 under those conditions, by dividing the extracellular $Ca^{2+}$ concentration (1.4 mM; Sandler and Kirschfeld, 1991) with the product of the maximal value of $Ca_i$ (20 $\mu$M) and the ratio of intracellular to extracellular volume (6.3; Sandler and Kirschfeld, 1991). Hereby we assume again that the following conditions hold: (1) there is no extracellular $Ca^{2+}$ buffering; (2) the glial cells do not participate in the $Ca^{2+}$ homeostasis; (3) there is no substantial $Ca^{2+}$ release from internal stores. Therefore, the important point that we wish to emphasize here is that the ratio of buffered to free calcium very likely is not constant and this limitation of the buffering capacity results in high $Ca_i$ values in bright light. This conclusion is not affected by the uncertainties in calculated values for $B_{inf}$.

Another possible reason for the high discrepancy between the values for $B_{inf}$ derived here and those reported by Hardie (1996a) is the different method. The estimate of Hardie (1996a) is based on the ratio of influx (measured by integrating the current) to free $Ca_i$ measured with optical methods.

Any $Ca^{2+}$ extruded in the period of integrating the current (possibly by the $Na^+/Ca^{2+}$ exchanger) contributes to the buffering, while in our approach, this $Ca^{2+}$ reappears in the extracellular space, and thus does not contribute to the buffering. Therefore our values are necessarily lower than the estimate made by Hardie (1996a).

Probably, there are many different buffer mechanisms with different affinities and capacities. However, it is possible to calculate the parameters of a single, equivalent buffer from the values of Figure 2.7c. We have fitted the data points of Figure 2.7c to a simple buffer model, taking

$$\frac{\mathrm{Ca_{tot}}}{\mathrm{Ca_i}} = 1 + \frac{B}{K_d + \mathrm{Ca_i}}$$

where $\mathrm{Ca_{tot}}$ is the total $Ca^{2+}$ concentration and $B$ the total concentration of a buffer with dissociation constant $K_d$. The buffering coefficient of the $Ca^{2+}$ influx ($B_{\mathrm{inf}}$) was calculated by

$$B_{\mathrm{inf}}(I) = \frac{\mathrm{Ca_{tot}}(I) - \mathrm{Ca_{tot,da}}}{\mathrm{Ca_i}(I) - \mathrm{Ca_{i,da}}}$$

where $\mathrm{Ca_{tot,da}}$ is the total $Ca^{2+}$ concentration in the dark. The smooth line in Figure 2.7c was obtained by taking $B = 18$ $\mu$M and $K_d = 0.77$ $\mu$M.

### *Comparison with other cellular processes dependent on calcium*

Illumination of invertebrate photoreceptors with bright light induces a rapid activation of mitochondrial respiration, presumably due to a rise in $\mathrm{Ca_i}$ (Fein and Tsacopoulos, 1988). In the white-eyed blowfly mutant *chalky*, illumination causes a rapid change in the redox state of mitochondrial flavoproteins (Stavenga and Tinbergen, 1983). A comparison of the intensity dependence of this process (Mojet et al., 1991) with the present calcium measurements yields that the transient shift in the redox state of flavoproteins occurs when $\mathrm{Ca_i}$ levels rise above $\sim$1 $\mu$M. At these concentrations, the mitochondria are indeed likely to take up considerable amounts of $Ca^{2+}$ (e.g. Miyata et al., 1991; Babcock et al., 1997).

The pupil mechanism of wild type fly photoreceptors, existing of pigment granules migrating inside the cell soma, has also a distinct dependence on $Ca^{2+}$ influx (Kirschfeld and Vogt, 1980; Howard, 1984; Hofstee and Stavenga, 1996). The measurements of the intensity dependence of this system, together with that of the receptor potential (Roebroek and Stavenga, 1990),

also show that the pupil gets activated at $Ca_i$ levels $\geq 1$ $\mu$M. In addition to increasing the signal to noise ratio of the receptor potential at high light intensities (Howard et al., 1987), the function of the pupil in wild type photoreceptors may therefore be to avoid very high $Ca_i$ levels.

A change in both the membrane potential and $Ca_i$ is caused by the same underlying event, i.e. a change in the permeability of the light activated channels. Curiously, whereas the plateau membrane potential saturates at $\log I \approx$ 1-2, $Ca_i$ shows a continous rise with intensity (Figure 2.6). Apparently, the light-dependent permeability increases with illumination intensity even at the brightest light intensities. Because buffering becomes minimal with large calcium loads, i.e. $Ca_i > 10$ $\mu$M (Figure 2.7), the rise in light-dependent permeability translates superlinearly into a rise in $Ca_i$. In addition, high $Ca_i$ possibly activates a $K^+$ conductance (Weckström, 1989) resulting in a reduced rise in membrane potential.